Catena 270 (2026) 110175

Contents lists available at ScienceDirect

Catena

journal homepage: www.elsevier.com/locate/catena

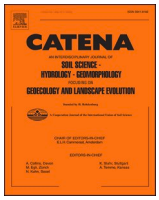

HYGRID-M: A grid-based hydrological balance model for water management at River Basin District scale

Htay Htay Aung [a,*], Biagio Sileo [a], Mauro Fiorentino [b], Silvano Fortunato Dal Sasso [a]

[a] Department of Humanistic, Scientific and Social Innovation (DiUSS), Università degli Studi della Basilicata, 75100 Matera, Italy
[b] Department of Engineering (DiING), Università degli Studi della Basilicata, 85100 Potenza, Italy

ARTICLE INFO

Keywords:
Water balance modeling
Actual evapotranspiration
Runoff
Soil heterogeneity
Dynamic land use

ABSTRACT

Accurate water balance estimation is crucial for sustainable water management, particularly under increasing climate variability. This study presents HYGRID-M, a monthly grid-based hydrological model developed in Python for the River Basin District (RBD) scale. Its main advantages lie in (i) explicit representation of spatial heterogeneity in soil properties derived from dynamic land use, (ii) the application of a temperature-based Hargreaves evapotranspiration formulation tailored to Mediterranean climatic conditions. The model was applied to the Southern Apennines District in Italy (2000−2023), where soils and land use are highly heterogeneous and temperature-driven evapotranspiration plays a dominant role. When validating the modeled AET against estimates from GLASS, ETMonitor, and MOD16, the HYGRID-M model exhibited significant agreement with MOD16 followed by ETMonitor and GLASS. Including heterogeneous soil depths derived from dynamic land use data and a regionalized Hargreaves coefficient for southern Italy significantly improved AET accuracy. Moreover, Q estimates closely aligned with precipitation forcing and were comparable to BIGBANG outputs. The model further revealed its sensitivity to the spatial heterogeneity in soil properties in estimating Q at the RBD scale. At the basin scale, the calibrated runoff coefficient (β) improved the model performance with KGE and NSE reaching 0.87 and 0.89, indicating the transferability of the model from the RBD to basin scales. Overall, these results demonstrated HYGRID-M's potential as a reliable tool for water management in Mediterranean climate-sensitive regions.

1. Introduction

The Mediterranean region is widely recognized as a climate change hotspot, with future projections indicating rising temperatures and declining annual precipitation, leading to significant reductions in water availability and increased drought frequency (Mariotti et al., 2008; Peres et al., 2023; Senatore et al., 2011). Southern Italy, which is part of the Mediterranean region, has already experienced recurring severe drought events (2002, 2007, 2008, 2011, 2017), primarily driven by its complex hydrogeological setting and the interaction between precipitation and recharge processes (Braca et al., 2019, 2022). These climatic trends are intensifying water scarcity; making accurate quantification of water balance components at the RBD scale essential for sustainable water resource management (Braca et al., 2019; Rautela et al., 2024, 2025a, 2025b).

Water balance models have been developed across a range of temporal scales such as hourly, daily, monthly, and yearly as well as spatial scales, including event-based, catchment, regional, and global levels, to estimate key water balance components (Braca and Ducci, 2018; Braca et al., 2022; Grogan et al., 2022; Mammoliti et al., 2021). Among these, monthly water balance models, first introduced by Thornthwaite (1948); have been widely adopted and further modified to address various hydrological problems (Thomas Jr, 1981; Wang et al., 2011; Zhang et al., 2008). They have proven to be valuable tools for assessing the hydrological characteristics of diverse river basins and for evaluating the impacts of climate change on hydrological regimes (Xu and Singh, 1998). These models typically require limited input parameters; such as monthly precipitation; temperature; and potential evapotranspiration; making them computationally efficient. Their low data demand and fast runtime allow for extensive simulations across various spatial scales ranging from basin to regional and even global levels (Wang et al., 2011). Moreover; they represent relatively simple

* Corresponding author.
E-mail addresses: htay.aung@unibas.it (H.H. Aung), biagio.sileo@unibas.it (B. Sileo), mauro.fiorentino@unibas.it (M. Fiorentino), silvano.dalsasso@unibas.it (S.F. Dal Sasso).

https://doi.org/10.1016/j.catena.2026.110175
Received 13 November 2025; Received in revised form 20 April 2026; Accepted 26 April 2026

hydrological processes and often require only a small number of parameters. This simplicity facilitates easier calibration in gauged catchments and enables parameter estimation through regionalization in ungauged basins (Wang et al., 2011).

These monthly water balance models have also been incorporated into spatially distributed frameworks for surface and groundwater modeling, such as WetSpass_M (Abdollahi et al., 2017; Amiri et al., 2022), WetSpass (Batelaan and De Smedt, 2001; Xu and Singh, 1998), USGS monthly water balance model (Wieczorek et al., 2022) and BIGBANG (Braca and Ducci, 2018; Braca et al., 2022). Although monthly grid-based water balance models are widely used for regional hydrological assessment due to their computational efficiency and low data requirements, they are often based on highly simplified and structurally rigid assumptions, including uniform soil water storage capacity across the domain and non-regionalized evapotranspiration formulations. Several parameters lack a clear physical interpretation because the model structure is predefined prior to any modeling (Pechlivanidis et al., 2011). As a result, their ability to realistically represent spatial heterogeneity and key hydrological processes is often limited (Kumar et al., 2024). In contrast, physically based or semi-distributed models such as SWAT (Arnold et al., 2000); VIC (Liang and Lettenmaier, 1994); HBV (Bergström, 1975) and WBM (Grogan et al., 2022) can explicitly simulate spatial variability and complex process interactions; but this comes at the expense of requiring extensive input data; hundreds of parameters; intensive calibration efforts; and significantly higher computational costs (Abdollahi et al., 2017). Consequently, these models often allow different parameter sets to produce similar results and tend to transfer poorly, especially at larger scales. Therefore, a key gap remains between the simplicity and efficiency of traditional monthly grid-based models and the more physically realistic but complex distributed approaches, particularly for operational water balance assessments at the RBD scale.

The HYGRID-M (an acronym for HYdrological GRIDed – Monthly) addressed this gap by introducing two key refinements within the monthly grid-based framework: (i) explicit representation of soil heterogeneity derived from dynamic land use and (ii) a regionalized temperature-driven evapotranspiration formulation adapted to Mediterranean hydroclimatic conditions. The aim of this study is to refine the modeling structure to incorporate soil heterogeneity and regionalized parameter on water balance calculations while maintaining low dependence on calibration, providing a tool for sustainable water management under changing climate conditions. The study has two main objectives: (1) evaluating the performance of the HYGRID-M model at the RBD scale, and (2) assessing its transferability to the basin scale for water balance prediction.

2. Materials and methods

2.1. Case study

The model was implemented in the Southern Apennines River Basin District (Fig. 2), which covers an area of approximately 68,200 km^2 and spans seven administrative regions in Italy, Basilicata, Calabria, Campania, Molise, and Puglia, as well as portions of Abruzzo and Lazio.

It represents one of the most hydro-geologically complex regions of the Italian peninsula. The territory is characterized by marked geomorphological diversity, ranging from mountainous and hilly sectors of the Apennine chain to extensive lowland plains such as the Tavoliere Plain (Puglia), the Metaponto Plain (Basilicata), and the Sibari Plain (Calabria). The Apennine ridge, extending predominantly in a north–south direction, separates the Tyrrhenian and Adriatic slopes and exhibits a complex structural setting that leads to strong variability in lithology and permeability. This heterogeneity controls the distribution and geometry of hydrogeological structures and influences groundwater circulation patterns across multiple spatial scales. The river network is generally dense and articulated, including perennial rivers, ephemeral streams, and fiumare.

From a hydro-climatic and hydrological perspective, the study area exhibits pronounced spatial gradients that translate into markedly different runoff responses. The regional climate ranges from dry subhumid Mediterranean conditions in the lowlands of Puglia to more humid, mountain-influenced regimes in Basilicata, Campania, and Calabria, with precipitation mainly concentrated in the autumn–winter season and pronounced summer dryness in lowland sectors. This climatic variability, combined with differences in soil storage capacity, topography, and lithological controls, results in the coexistence of infiltration-excess (Hortonian) dominated responses in drier, low-storage basins and saturation-excess mechanisms (Dunnian) in more humid, mountainous catchments.

2.2. HYGRID-M model

The HYGRID-M model was developed at the RBD scale, featuring 1-km spatial resolution and monthly temporal resolution. The model was implemented following the approach of the BIGBANG model (Braca and Ducci, 2018) in conjunction with the Thornthwaite monthly water-balance model (McCabe and Markstrom, 2007; Thornthwaite, 1948). Developed within a Python programming environment, the model was designed to simulate key hydrological processes including snowmelt (Snowmelt), actual evapotranspiration (AET), runoff (Q), surplus (S), and water deficit (DF) at the scale of individual grid cells by incorporating climatic data such as precipitation, temperature, and soil moisture characteristics. The governing equation of the model is based on the mass balance written for i^{th} month as follows:

$$P_i - AET_i - Q_i = \Delta ST_i \tag{1}$$

The amount of monthly precipitation P_i in the form of rain ($P_{rain,i}$) or snow ($P_{snow,i}$) is estimated in the monthly interval. Precipitation can be considered as snow if the monthly mean temperature (T_i) is greater than a specified threshold T_{snow}, and as rain if it is greater than another specified threshold T_{rain}. The amount of snow precipitation linearly decreased from 100 to 0% based on these threshold values, which is expressed as follows:

$$Snow_i = \begin{cases} 1 \text{ if } T_i > T_{snow} \\ \dfrac{T_{rain} - T_i}{T_{rain} - T_{snow}} \text{ if } T_{snow} \le T_i \le T_{rain} \\ 0 \text{ if } T_i < T_{rain} \end{cases} \tag{2}$$

McCabe and Markstrom (2007) recommended that T_{snow} can express two different values based on elevation (Z) as follows:

$$T_{snow} = \begin{cases} T_{snow,sup} \text{ if } Z > Z_{snow} \\ T_{snow,inf} \text{ if } Z \le Z_{snow} \end{cases} \tag{3}$$

Following Braca and Ducci (2018) and McCabe and Markstrom (2007); T_{rain} as 3.0 °C; $T_{snow;sup}$ as −10.0 °C; $T_{snow;inf}$ as −1.0 °C and Z_{snow} as 1000 m above mean sea level (m.s.l) are adopted. Snowmelt was estimated using the simple degree-day method which assumes an empirical relationship between snowmelt and monthly mean temperature (Hock, 1999; USDA - United States Department of Agriculture, 2004) as follows:

$$Snowmelt_i = \begin{cases} c \times (T_i - T_{snowmelt}) \text{ if } Z > Z_{snow} \\ 0 \text{ if } Z \le Z_{snow} \end{cases} \tag{4}$$

where c is adopted as 150 mm/^{0}C/month and $T_{snowmelt}$ as 0 °C, following Braca and Ducci (2018). The parameter c; representing the melt-rate factor; typically ranges from 1.6 to 6 mm/^{0}C/day (50 to 180 mm mm/^{0}C/month) according to USDA - United States Department of Agriculture (2004). In this study; the above value was adopted for the Italy based on Braca and Ducci (2018). The model adopted the direct runoff ($Q_{d;i}$); which derives from impervious surfaces or infiltration-excess overflow; as the fraction of $P_{rain;i}$; 5%; which is the direct

runoff coefficient (*SRC*) adopted in this study (Wolock and McCabe, 1999).

The actual evapotranspiration (AET_i) can be satisfied by the reference crop evapotranspiration (ETo_i) and soil water storage (ST_i). In the model, ETo_i representing as a key component of the hydrological balance is implemented. ETo_i was computed based on the Hargreaves equation (Hargreaves and Samani, 1985), which is a temperature-based, and the expression is described as follows:

$$ETo_i = C\ M\ R_a(T_i + 17.8)\sqrt{\Delta T_i} \tag{5}$$

where R_a (mm/day) is the water equivalent of extraterrestrial radiation (depending on the inverse relative Earth-Sun distance, the sunset hour angle, the latitude, and the solar declination); M is the number of the day in each month; ΔT_i (°C) is the monthly temperature range; and C is the generalized Hargreaves coefficient which is set to 0.0023. Mendicino and Senatore (2013) recalibrated the Hargreaves coefficient for Southern Italy and proposed a regionalized formulation; as expressed in Eq. (6). Their findings demonstrated that the Hargreaves equation incorporating the regionalized coefficient outperformed the original equation; yielding improved estimation accuracy across various applications in Mediterranean regions (Senatore et al., 2015; Senatore et al., 2020). Notably, the equation exhibited better performance when applied at the daily scale compared to the monthly scale. The regionalization of the Hargreaves coefficient is based on the formulation of a suitable mathematical equation linking it to $\overline{T_i}$ and $\overline{\Delta T_i}$, which are average values of T_i and ΔT_i. The equation for a regionalized coefficient based on a quadratic regression related to $\overline{\Delta T_i}$ is expressed as follows.

$$C = 1.23057 \times 10^{-5}\ \overline{\Delta T_i}^{2} - 3.9237 \times 10^{-4}\overline{\Delta T_i} + 4.8026 \times 10^{-3} \tag{6}$$

AET_i has the upper limit which is ETo_i. However, if total inflow ($P_{total,i}$) is not sufficient to meet atmospheric demand, the deficit is compensated by withdrawing the water from the soil moisture of the previous month ($ST_{i\text{-}1}$). Thus, AET_i is determined by $P_{total,i}$, ETo_i, soil water storage (ST_i), and soil water withdrawal (STW_i). In other words, when total inflow ($P_{total,i}$) is less than ETo_i, AET_i is equal to $P_{total,i}$ plus the amount of soil water that is withdrawn from soil-water storage; otherwise, AET_i is equal to ETo_i.

$$AET_i = \begin{cases} P_{total,i} + STW_i \text{ if } P_{total,i} \le ETo_i \\ ETo_i \text{ if } P_{total,i} > ETo_i \end{cases} \tag{7}$$

$P_{total,i}$ is obtained from the part of monthly precipitation in the form of rain and snowmelt, and soil water storage and soil-water storage withdrawal are computed as follows:

$$ST_i = ST_{i-1} - \left[\left| P_{total,i} - ETo_i \right| \times \left(\frac{ST_{i-1}}{ST_{max}} \right) \right] \tag{8}$$

$$STW_i = ST_i - ST_{i-1} \tag{9}$$

where ST_{max} is the maximum soil water storage capacity; and ST_{i-1} is the soil water storage for the previous month. ST_{max} is expressed as follows:

$$ST_{max} = (\theta_{fc} - \theta_{wp})D \tag{10}$$

where θ_{fc} is the moisture storage at field capacity, θ_{wp} is the moisture storage at wilting point, and D is the rooting depth. The water deficit (DF) in this model is computed by subtracting AET_i from ETo_i.

Soil moisture is determined by ST_{max} and after the soil moisture reaches to its full capacity (i.e. ST_{max}), the excess water is assumed to contribute to outflow to the river. In the model, when $P_{total,i}$ exceeds ETo_i, the excess water obtained from the difference between $P_{total,i}$ and ETo_i replenishes ST_i. When ST_i is greater than ST_{max}, the excess water is obtained as the surplus (S_i). Here, the total surface runoff can be computed from the direct runoff ($Q_{d,i}$) and fraction of S_i. The runoff coefficient (β) is the fraction of the surplus in the generation of the total surface runoff and it is generally set to 0.5 (McCabe and Wolock, 2011; Wolock and McCabe, 1999). The runoff factor is strictly related to the percentage of impermeable areas and different climatic regions (Boughton, 1987; Longobardi et al., 2003). The surface runoff ($Q_{s,i}$) and the relationship of total runoff (Q_i) can be expressed as follows:

$$Q_{s,i} = \beta \times (S_i + S_{i-1}) \tag{11}$$

$$Q_i = Q_{d,i} + Q_{s,i} \tag{12}$$

Fig. 1 presents the hydrological factors evaluated at each grid cell and the detailed computation structure of the HYGRID-M model. The default values and allowable ranges of each model parameter employed in the HYGRID-M model are listed in Table A1 in Appendix A.

2.3. Datasets

This study used hydrological variables, soil depths, Digital Elevation Model (DEM), and land cover information as input forcings for the HYGRID-M model. All input datasets were processed to a 1-km resolution based on the bilinear interpolation within a grid-based framework referenced to the ETRS89 datum, same as the one in the BIGBANG model. The simulation covered a 24-year period from 2000 to 2023. Moreover, multiple global datasets were used to comprehensively evaluate the actual evapotranspiration estimated by the newly proposed HYGRID-M model and the BIGBANG model for the Southern Apennines District. Table 1 provides an overview of the global datasets used and datasets from the BIGBANG model. All datasets, except MOD16 which has a spatial resolution of 500 m, were aggregated to a monthly time step.

2.3.1. Model inputs

The simulation used key input hydrological variables: total precipitation and mean temperature from SINAnet (ISPRA) (https://groupware.sinanet.isprambiente.it/bigbang-data/library/bigbang_80), along with maximum and minimum temperatures obtained from SCIA (ISPRA) (https://scia.isprambiente.it/servertsdailyutm/serietemporalidaily400.php) from 2000 to 2023. A high-resolution DEM, derived from the EU-DEM v1.1 (https://land.copernicus.eu/imagery-in-situ/eu-dem/eu-dem-v1.1) provided by the Copernicus Land Monitoring Service (CLMS). Land use and land cover information was taken from the CORINE Land Cover database (EEA, 2018) (https://land.copernicus.eu/en/products/corine-land-cover). Pedological information was derived from maps provided by the European Soil Data Centre (ESDA) (https://esdac.jrc.ec.europa.eu) (Ballabio et al., 2016); with particular reference to physical properties such as soil texture (percentages of sand; silt; and clay) and organic matter content. Soil hydraulic properties were then estimated using pedotransfer functions (Saxton and Rawls, 2006). In this approach; both the field capacity and the wilting point were computed as functions of the weight percentages of sand; clay; and organic matter derived from the distributed TOPSOIL property maps. Finally; in order to account for spatial heterogeneity in soil water storage capacity; CORINE land cover classes were reclassified into 17 categories (Hlavčová et al., 2008; Liu and De Smedt, 2004), each assigned root depth from literature. For consistency with HYGRID-M, these were further aggregated into five main land use classes: forest, grassland, cropland, bare soil, and impervious areas. Soil depths were derived for four separate years (2000, 2006, 2012 and 2018) based on the information of CORINE datasets. Details of datasets can be found in Table A2 in the Appendix A.

2.3.2. GLASS dataset

The GLASS ET Product Version 5.0 (v5.0) uses a deep neural network (DNN) merging framework to improve terrestrial ET estimates by combining five satellite-derived ET products: MOD16 (MODIS), SW (Shuttleworth–Wallace), PT-JPL (Priestley–Taylor), MS-PT (modified Priestley–Taylor), and simple hybrid SIM (Xie et al., 2022). Each ET model's inputs included 1-km spatial resolution and 8-day temporal resolution of GLASS vegetation and radiation datasets: fraction of

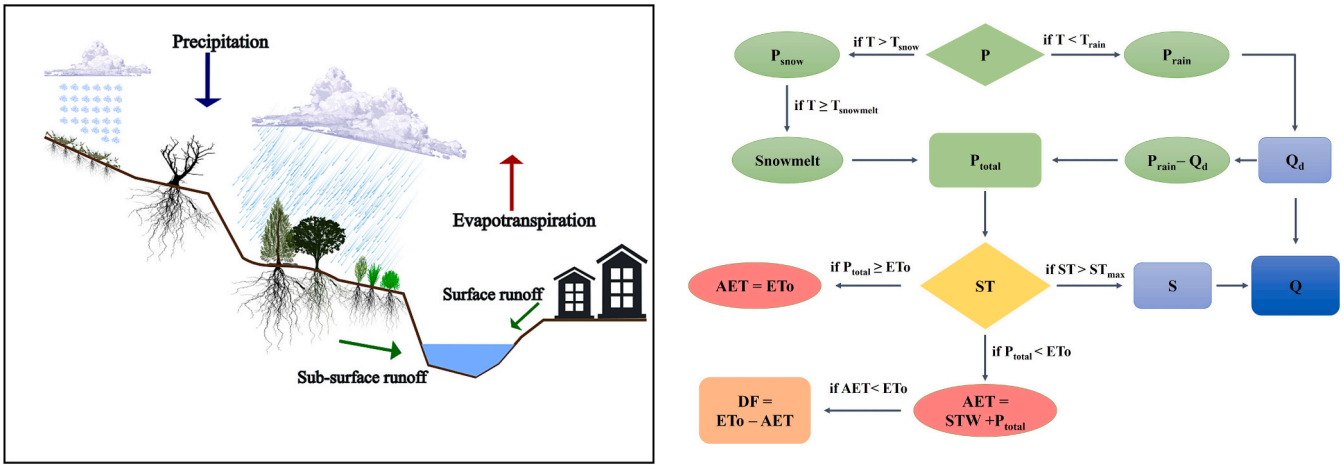

Fig. 1. (a) Conceptual representation of the hydrological system at grid scale in the study area, showing the interaction between the main components of the water cycle in a Mediterranean hydro-climatic context and (b) detailed computational structure of the HYGRID-M model.

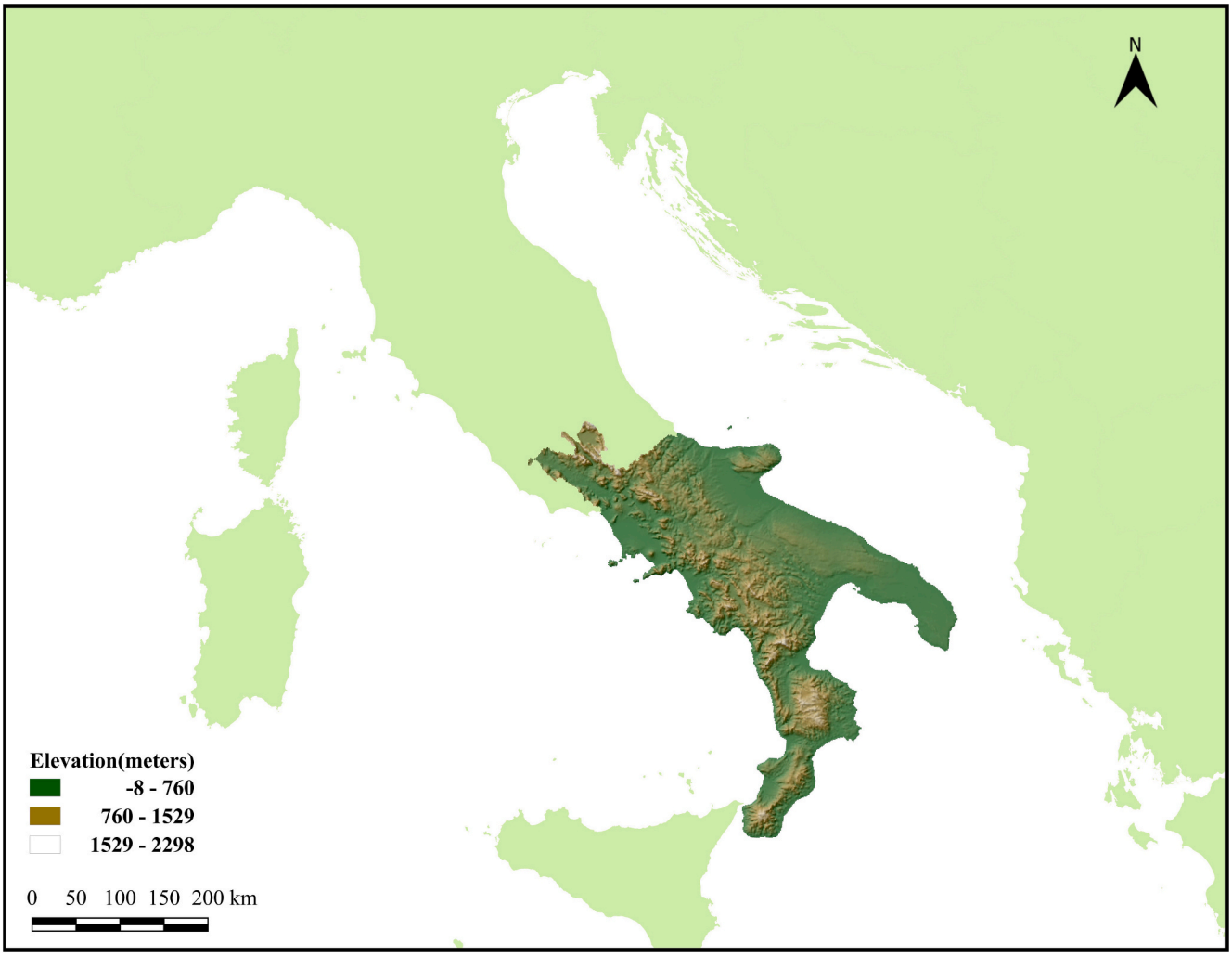

Fig. 2. Southern Apennines District in Italy.

absorbed photosynthetically active radiation (FPAR), leaf area index (LAI), normalized difference vegetation index (NDVI) products and daily R_n with a 0.05° alongside meteorological forcing such as air temperature (T_a), diurnal air temperature range (DT), relative humidity (RH), wind speed (WS), and soil moisture (SM). The dataset has a temporal resolution of an 8-day average and a spatial resolution of 1 km, mapped in the Sinusoidal (SIN) projection (scale factor 0.01), originally in W/m^2 and converted to mm/day using 1 W/m^2 = 0.035 mm/day.

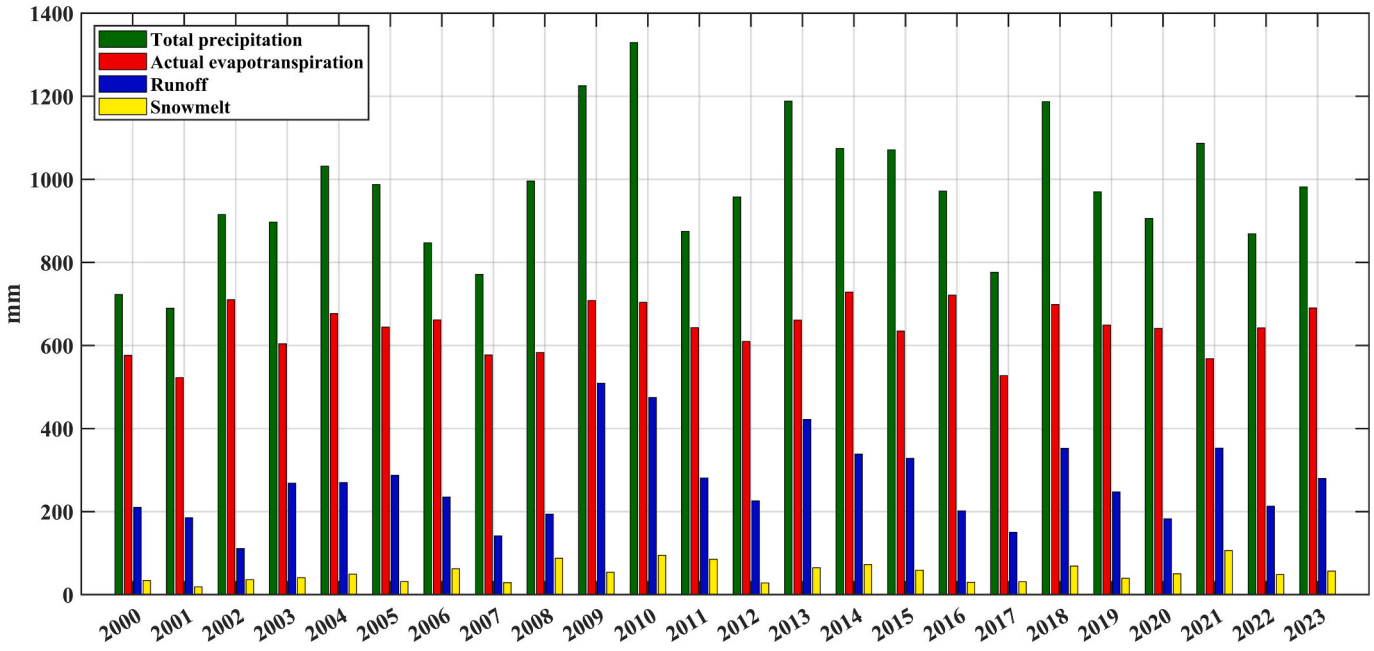

Fig. 3. Annual water balance components simulated by HYGRID-M for the period 2000–2023. Bars show total precipitation (green), actual evapotranspiration (red), runoff (blue), and snowmelt (yellow). (For interpretation of the references to colour in this figure legend, the reader is referred to the web version of this article.)

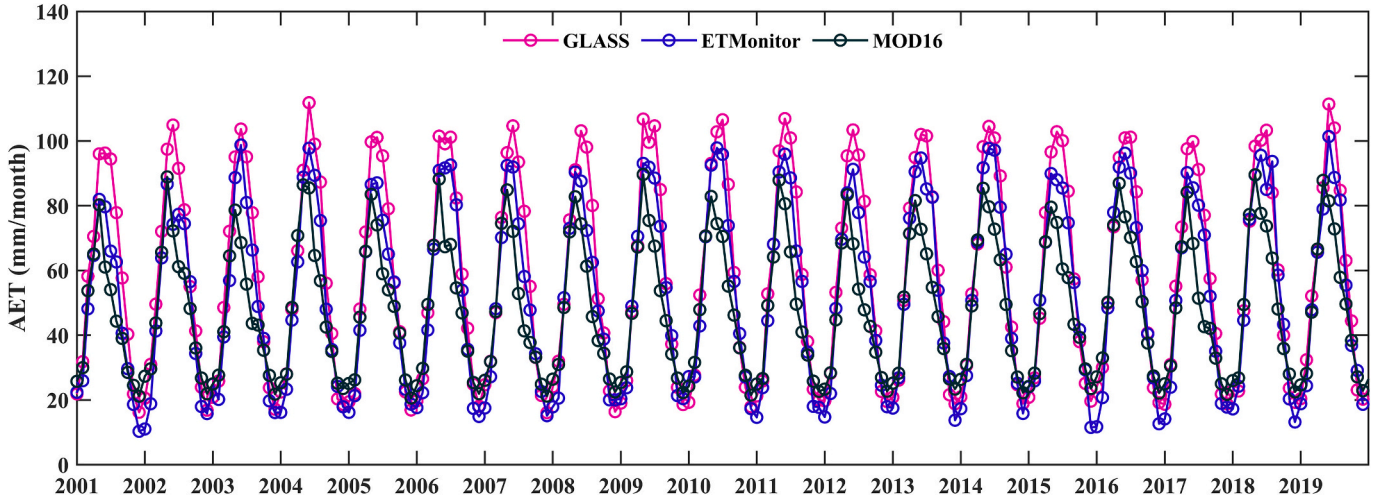

Fig. 4. Monthly average AET of GLASS, ETMonitor and MOD16 over Southern Apennines District from 2001 to 2019.

2.3.3. *ET monitor dataset*

The ETMonitor model employs a multi-parameterization scheme to estimate the various components of ET including vegetation transpiration, canopy rainfall interception loss, soil evaporation, water surface evaporation, and snow and ice sublimation by coupling energy-balance, water-balance, and plant-physiology simulations that govern surface fluxes (Zheng et al., 2022a). Its global; gap-free ET dataset spans from 2000 to 2019 at a daily time step and 1-km spatial grid and is derived from multi-source satellite observations and atmospheric forcing data (Zheng et al., 2022b). For this study, the global monthly ET product aggregated from the daily values was used and scaled by a factor of 0.1.

2.3.4. *MOD16 dataset*

The MODIS global ET algorithm is part of NASA's Earth observing system for estimating ET from the Earth's land surface using MODIS remote sensing data for hydrological and ecological applications. By adapting the algorithm of Cleugh et al. (2007); which is based on the Penman–Monteith method; Mu et al. (2007, 2011) developed the MOD16 ET product. The MOD16 ET algorithm operates on a daily basis; with daily ET calculated as the sum of daytime and nighttime ET. It accounts for water vapor fluxes from three sources: soil evaporation; wet canopy evaporation; and plant transpiration from dry canopy surfaces. According to Mu et al. (2007, 2011); ET is estimated using a combination of remote sensing inputs such as land cover; LAI; albedo; and FPAR along with global meteorological data. In this study; the 8-day composite MOD16A2GF product was used (Running et al., 2021). This year-end gap-filled dataset provides ET values in (kg/m^2/8day), is available from the year 2000 to the present, and has a spatial resolution of 500 m, mapped in the SIN projection with a scale factor of 0.1.

2.3.5. *BIGBANG dataset*

BIGBANG datasets were extracted from the BIGBANG (Italian acronym for “Bilancio Idrologico GIS BAsed a scala Nazionale su Griglia regolare”) model, that was developed by ISPRA to evaluate the water

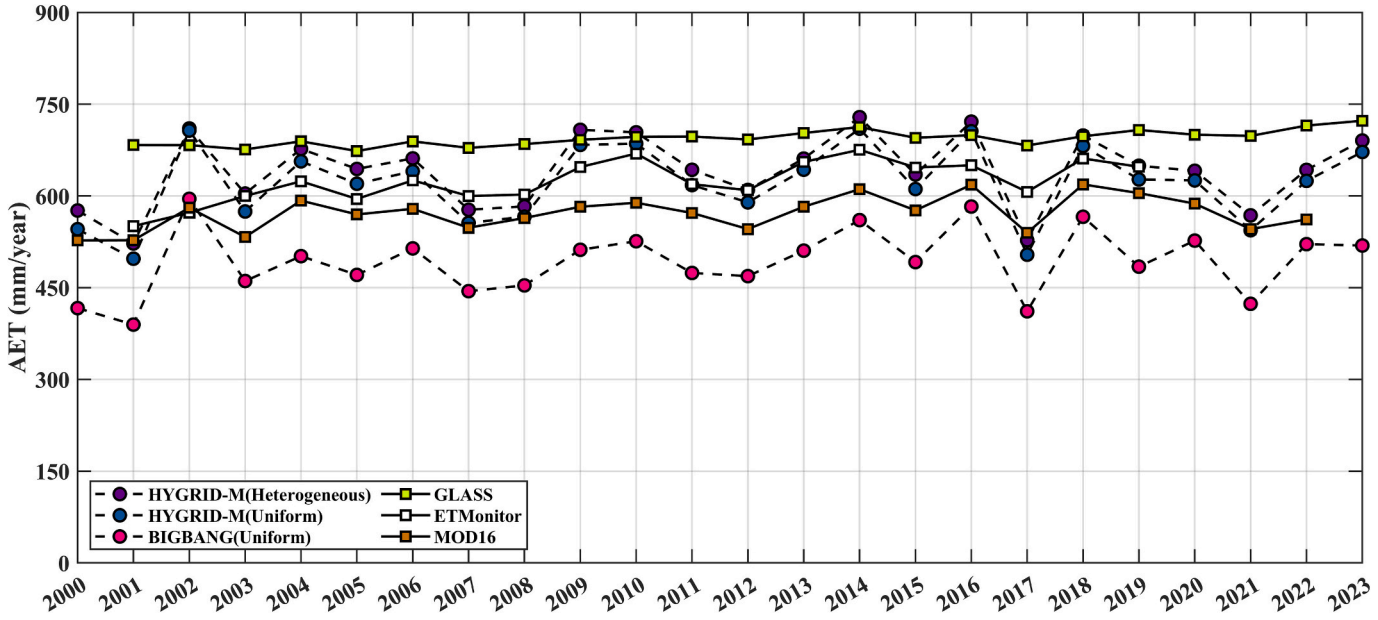

Fig. 5. Comparison of average annual AET over Southern Apennines with GLASS (2001−2023), ETMonitor (2001–2019), and MOD16 (2000−2022).

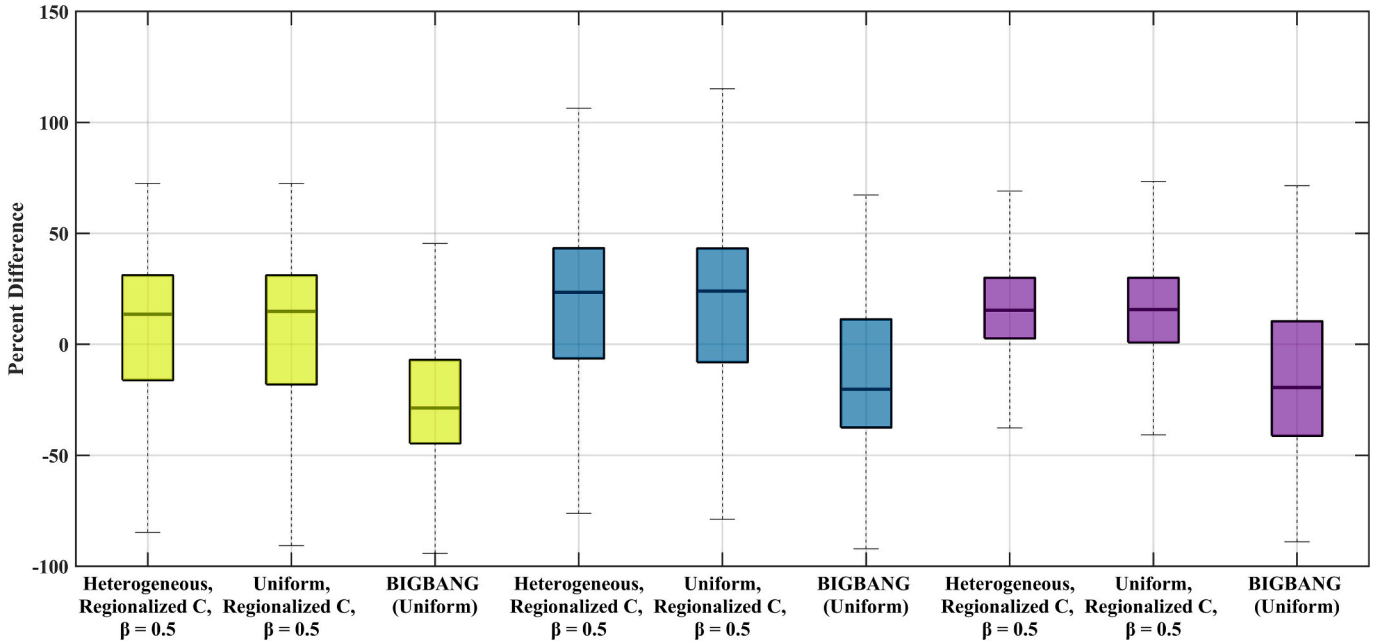

Fig. 6. Percent differences in monthly AET over Southern Apennines with reference to GLASS (2001–2023), ETMonitor (2001–2019), MOD16 (2000–2022) [yellow colour referred to comparison with GLASS, blue to ETMonitor and purple to MOD16]. (For interpretation of the references to colour in this figure legend, the reader is referred to the web version of this article.)

balance components at a monthly temporal scale and a 1-km spatial scale. It is implemented on a proprietary GIS platform using Python, within the ETRS89 datum and the Lambert Azimuthal Equal-Area (LAEA) projection, as adopted by the European Environment Agency. The model applies the Thornthwaite-Mather mass-balance approach to simulate precipitation, actual evapotranspiration, surface runoff, groundwater recharge, and changes in soil/snow storage for each grid cell (Braca and Ducci, 2018; Braca et al., 2022). Soil moisture is represented by a 1-m deep reservoir, whose maximum storage (AWS) is derived from LUCAS based soil texture metrics (sand, silt, clay) applied across the domain (Tóth et al., 2013). When precipitation exceeds AWS; the surplus is partitioned between recharge and surface runoff based on a Potential Infiltration Coefficient (PIC). PIC values are assigned according to geological permeability classes; using updated ISPRA permeability mapping for improved spatial detail. Model calibration and validation are limited in previous applications but specific regional case studies; such as Campania (1996–2015); suggest that modeled recharge and runoff compare reasonably with local-scale data (Braca et al., 2019). Recent evaluations also indicate that the adoption of the new permeability map reduces long-term national average recharge by ~6%; while increasing runoff (Braca et al., 2019). AET and Q estimates from the model over the study area are extracted for the model comparison.

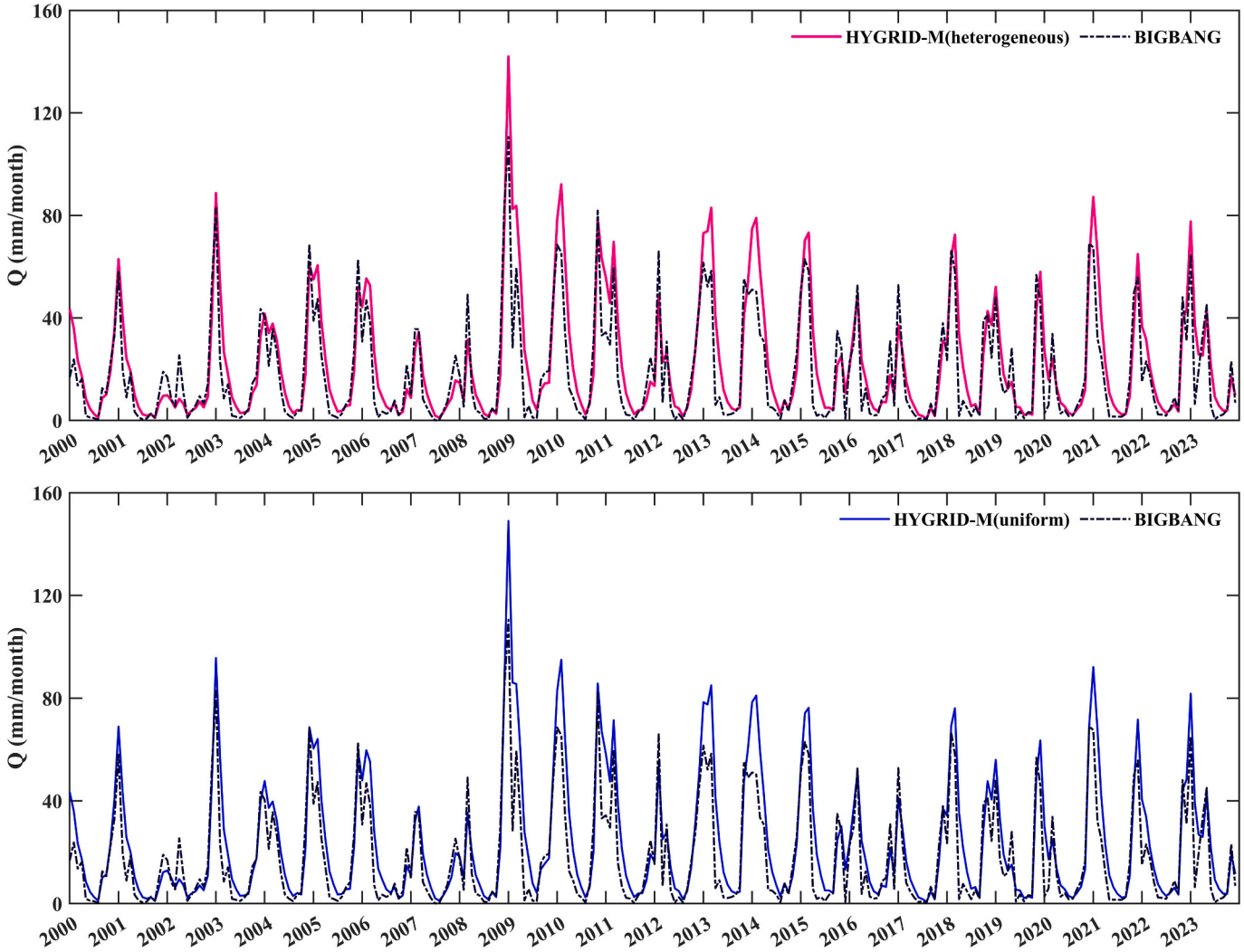

Fig. 7. Comparison of monthly average Q estimates by the HYGRID-M model under (a) heterogeneous and (b) uniform soil conditions and the BIGBANG model over the Southern Apennines for the period 2000–2023.

2.4. Model evaluation

The overall model evaluation was based on the comparison with multiple independent datasets to assess the performance of the proposed HYGRID-M model at both RBD scale and basin scale. At the RBD scale, AET estimates were evaluated with three global ET products (GLASS, ETMonitor, MOD16) and BIGBANG estimates, whereas Q estimates were assessed against BIGBANG simulations, as it represents the only national-scale monthly grid-based water balance model developed for Italy at the same spatial resolution (1 km) and based on a similar concept. At the basin scale, β was tested within a plausible range (0.3–0.7) to evaluate how regional-scale parameterization transfers to basin scale under varying hydrogeological conditions, based on observed discharge data from 11 pilot basins distributed across the Southern Apennines District (Xiao et al., 2020).

Model performance was quantified using multiple statistical metrics, including the correlation coefficient (R), Kling–Gupta Efficiency (KGE) (Gupta et al., 2009); Nash-Sutcliffe efficiency (NSE) (Nash and Sutcliffe, 1970); Root Mean Square Error (RMSE); and the *p*-value (*p*). The correlation coefficient (R) indicates the consistency between the simulated and observed values. The NSE is employed to evaluate the model's predictive skill. The KGE extends the NSE framework by decomposing model performance into three components: correlation; variance and mean bias. The RMSE is commonly employed error metrics that quantify the average magnitude of prediction errors. The p-value is the probability of obtaining the results at least as extreme as one of the observed values; that indicates the statistical significance. KGE and NSE were chosen as the primary performance metrics because they provide a comprehensive assessment of correlation; bias; and variability between simulated and reference values. In particular; KGE has proven particularly effective in reproducing the magnitude and variability of hydrological extremes (Dal Sasso et al., 2025; Mizukami et al., 2019). R was computed to quantify the linear relationship between observed and simulated values, while RMSE was used as a measure of absolute error.

3. Results

3.1. Assessment of actual evapotranspiration (AET)

The HYGRID-M model reproduces consistent interannual dynamics of AET over the period 2000–2023 (Fig. 3). AET closely follows precipitation variability, with higher values in wet years (e.g., 2009, 2014, 2016) and lower values in drier years (e.g., 2001, 2017). The spatial distribution of AET as well as other components (P_{rain}, P_{snow} and Q) at the monthly scale, provided in Appendix A, confirms the seasonal cycle, with minimum values in winter, a rapid increase in spring, a peak in early summer, and a marked decline under summer drought conditions.

The actual evapotranspiration estimated by the HYGRID-M model

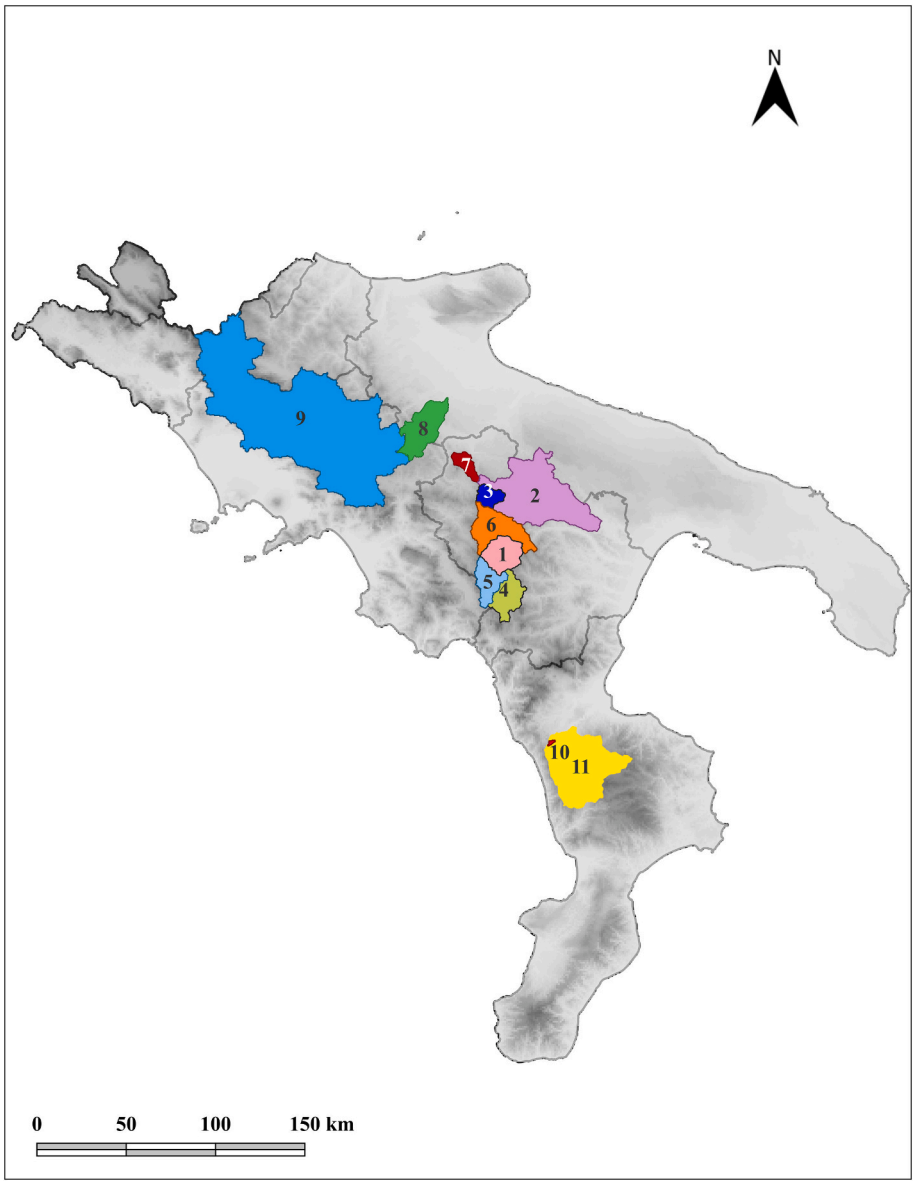

Fig. 8. Location of 11 pilot basins considered in this study.

was assessed on monthly and annual scales by comparing it with the retrieval AET of global products: GLASS, ETMonitor and MOD16, and the AET estimates from the BIGBANG model.

3.1.1. Cross comparison of global AET

Fig. 4 presents the monthly average AET estimates derived from the GLASS, ETMonitor, and MOD16 datasets over the Southern Apennines District for 2001–2019. Peak AET values occurred in June for both the GLASS and ETMonitor datasets, whereas the MOD16 dataset indicated an earlier peak in May. Among the three datasets, GLASS consistently reported the highest AET estimates, followed by ETMonitor and MOD16. The lowest AET values were observed in December and January across all datasets, with MOD16 exhibiting slightly higher values than both GLASS and ETMonitor during these months. It is noted that the Southern Apennines District exhibits higher AET during the summer period and lower AET during the winter period. The average peak AET values over the time series were 103.53 mm/month for GLASS (in June), 91.83 mm/month for ETMonitor (in June), and 84.67 mm/month for MOD16 (in May). In contrast, the lowest values occurred in January, with estimates of 21.38 mm/month for GLASS, 17.97 mm/month for ETMonitor, and 25.50 mm/month for MOD16. These differences indicate a degree of discrepancy among the global datasets.

3.1.2. Comparison of annual and monthly average AET with global datasets

Fig. 5 shows the annual average AET from the HYGRID-M model under heterogeneous and uniform soil conditions, the BIGBANG model and retrieved from global datasets for Southern Apennines District during 2000–2023. As shown in Fig. 5 that the annual trends produced by HYGRID-M and BIGBANG are relatively similar to MOD16 followed by ETMonitor while GLASS showed nearly constant values over the entire simulation period. The mean of annual average AET values over the time series were observed as 641.00 mm/year and 620.21 mm/year for the HYGRID-M model under heterogeneous and uniform soil conditions, 492.71 mm/year for BIGBANG, 694.29 mm/year for GLASS, 624.08 mm/year for ETMonitor and 572.01 mm/year for MOD16. It is noted that the mean value of average annual AET from GLASS datasets over 24 years was notably higher, exceeding ETMonitor by approximately 11.3% and MOD16 by about 21.4%, indicating a systematic tendency of GLASS to produce higher evapotranspiration estimates

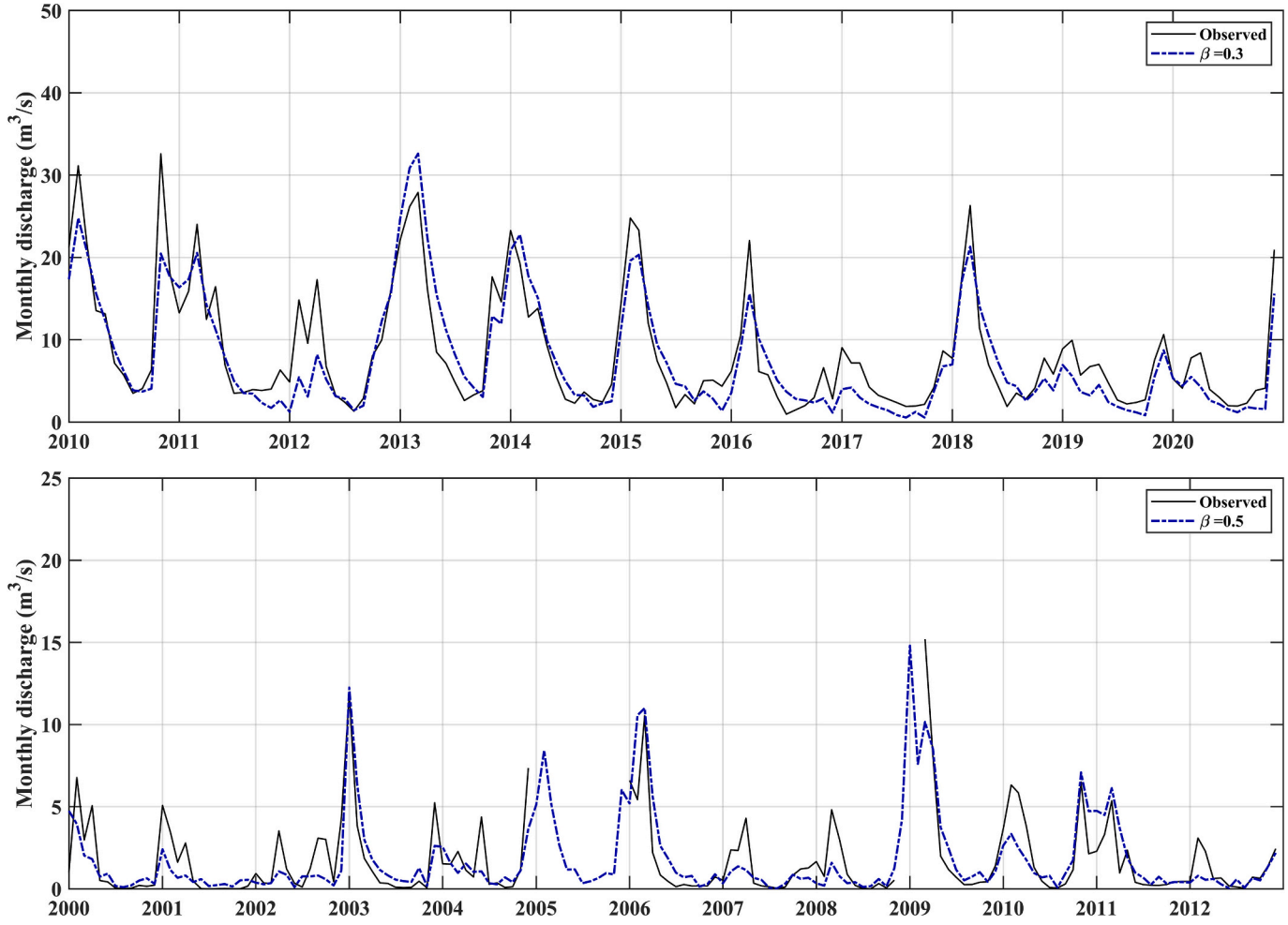

Fig. 9. Discharge comparison for (a) Agri at Pertusillo (a humid basin) and (b) Carapelle at Ponte Vecchio di Ordona (a semi-arid).

Table 1
Overview of global ET datasets and BIGBANG datasets used in this study.

Dataset	Time range	Spatial Resolution	Temporal resolution	Source
GLASS	2000–2023	1 km	8-day average	Xie et al. (2022)
ETMonitor	2000–2019	1 km	monthly	Zheng et al. (2022a, 2022b)
MOD16	2000–2022	500 m	8-day composite	Running et al. (2021)
BIGBANG	2000–2023	1 km	monthly	Braca and Ducci (2018)

compared to other reference datasets.

Annual average AET from the HYGRID-M model under heterogeneous soil condition shows comparable interdecadal variability, highlighting statistically significant correlations with GLASS ($R = 0.45$, $p < 0.03$), ETMonitor ($R = 0.67$, $p < 0.01$) and MOD16 ($R = 0.86$, $p < 0.01$). Similarly, AET estimates under uniform soil conditions also demonstrate significant correlations with GLASS (R = 0.45, $p < 0.031$), ETMonitor ($R = 0.64$, $p < 0.01$) and MOD16 ($R = 0.87$, $p < 0.01$). In comparison, AET from the BIGBANG model shows moderate correlations with GLASS ($R = 0.42$, $p < 0.044$), ETMonitor ($R = 0.55$, $p < 0.014$) and MOD16 ($R = 0.84$, $p < 0.01$). The average annual AET estimates from the HYGRID-M model were more closely correlated with those from the global datasets, whereas the BIGBANG model tended to produce comparatively lower values. The analysis showed that AET estimates by the HYGRID-M model under both soil conditions exhibited significant consistency with MOD16 datasets, achieving higher R and lower p while GLASS datasets produced relatively lower R and higher p values, indicating a lower statistical significance. Moreover, the analysis indicated that AET estimates by the HYGRID-M under heterogeneous soil condition differed from those under the uniform soil condition by about 3.2%, highlighting the influence of soil heterogeneity on AET in the study area. It is noted that among all reference datasets, GLASS shows the weakest statistical agreement with HYGRID-M and BIGBANG, whereas MOD16 demonstrates the highest level of statistical significance.

Under heterogeneous soil conditions, a linear regression over annual average AET revealed a positive trend of +1.5 mm per year, highlighting a progressive increase in water loss to the atmosphere. Interannual variability was marked: the driest years were 2001 and 2017 (−18 to −19% below the mean), while the wettest years were 2014 (+14%) and 2016 (+13%), with several others (2002, 2009, 2010, 2018, 2019, 2023) between +8% and + 11%; most years remained within ±10% of the average. Years such as 2007 and 2008, instead, showed moderately negative anomalies (about −5 to −7%), confirming a condition of relative deficit but without reaching the extremes of the series. The observed positive trend therefore reflects both climatic forcing and soil properties, with important implications for water availability, hydrological balances, and long-term water management strategies.

Fig. 6 illustrates the box plots of the monthly percentage differences in AET between the modeled outputs and three reference datasets: GLASS (2001–2023, yellow), ETMonitor (2001–2019, blue) and MOD16 (2000–2022, purple). The HYGRID-M model consistently showed the lowest median difference compared with the BIGBANG model, which was constrained to a uniform 1-m soil depth. The model obtained the

narrowest interquartile range (IQR) in comparison with MOD16, whereas the variability of monthly percentage differences was larger while comparing with GLASS and ETMonitor, highlighting significant correlation with MOD16 datasets. It is also noted that configurations using spatially heterogeneous soil depths led to narrower variations in AET differences than those assuming a uniform depth, indicating the benefit of accounting for spatial variability in soil properties. In contrast, the use of a regionalized versus generalized Hargreaves coefficient and variation of β had a minimal effect on the overall model performance at the monthly scale, although simulations based on the generalized coefficient produced slightly higher AET estimates during the summer months. The HYGRID-M model demonstrated stable and robust behavior across the tested configurations, with improved consistency in simulating AET dynamics.

Table 2 summarizes the statistical evaluation of the monthly average AET estimated by the HYGRID-M model under spatially heterogeneous and uniform soil depth conditions, as well as by BIGBANG, in comparison with the GLASS, ETMonitor, and MOD16 datasets. Compared to uniform soil depth assumptions, heterogeneous configurations improved agreement with reference AET datasets, reducing RMSE ~3 mm month^{-1}, respectively, and yielding higher R, and KGE values, indicating the satisfactory agreement of the model. The superior agreement of HYGRID-M with the MOD16 dataset (R = 0.84, KGE = 0.75) compared with GLASS and ETMonitor can be attributed to the model's explicit representation of soil moisture feedback and vegetation dynamics. MOD16, being a remote-sensing-driven product based on the Penman–Monteith approach, is particularly sensitive to spatial variations in rooting depth, soil water availability and land-use characteristics. By incorporating spatially heterogeneous soil storage capacity derived from dynamic land use and variable rooting depth, HYGRID-M better reproduces these surface controls, resulting in closer alignment with MOD16 than with the more aggregated GLASS and ETMonitor products. In contrast, the uniform 1-m soil depth assumption in the BIGBANG model leads to systematic underestimation of AET under Mediterranean conditions where evapotranspiration is strongly limited by soil moisture availability. Overall, the HYGRID-M model under heterogeneous soil depth conditions exhibits improved accuracy and consistency in estimating AET, outperforming both the HYGRID-M model at uniform soil depths and the BIGBANG model, particularly when evaluated against a high-resolution global ET product such as MOD16.

3.2. Assessment of runoff (Q)

The model was simulated based on the regionalized Hargreaves coefficient and β value of 0.5 for the entire period of 2000–2023. The available Q estimates from the BIGBANG model over the study area were compared with model outputs to assess the reliability of the HYGRID-M model in simulating of runoff generation. Fig. 7(a) illustrates the comparison of monthly Q values between the HYGRID-M model (heterogeneous soil conditions) and the BIGBANG model, whereas Fig. 7(b) presents the corresponding comparison for the HYGRID-M model under uniform soil conditions over the Southern Apennines District.

The runoff estimates produced by the HYGRID-M grid model under both heterogeneous and uniform soil conditions showed good overall agreement with those from the BIGBANG model at the RBD scale throughout the simulation period (2000–2023). Under heterogeneous soil conditions, the HYGRID-M model tends to overestimate certain higher peak flows, while the magnitude of some lower peaks appears to be less pronounced compared to the BIGBANG model. Consequently, the HYGRID-M model typically yielded higher runoff estimates throughout most of the simulation period. Similarly, under uniform soil conditions, the HYGRID-M model successfully captures all peak events identified by the BIGBANG model, with the corresponding peaks appearing more pronounced in this configuration. It is clear that the HYGRID-M model is sensitive to the spatial heterogeneity of soil properties, indicating its capacity to account for variations in soil depths. Moreover, the comparison with the available Q at the RBD scale highlighted that the proposed model performed well in estimating Q for Southern Apennines District.

3.3. Runoff comparison over basin scale

Discharge simulations produced by the model, under heterogeneous soil configurations, were evaluated against water balance-based discharge estimates for 11 pilot basins distributed across the Campania, Basilicata, Puglia, and Calabria regions (Fig. 8). For each basin, the optimal β was selected to ensure the best model performance, reflecting basin-specific hydrological characteristics. Table 3 summarizes the basin areas, metric values, and optimal β values of the HYGRID-M model, providing a clear basis for evaluating model performance across diverse climatic conditions. Fig. 9(a) and (b) present the discharge comparison for Agri at Pertusillo (a humid basin), and Carapelle at Ponte Vecchio di Ordona (a semi-arid).

In the Basilicata region, which encompassed both humid and semi-arid conditions, six pilot basins were analyzed. The HYGRID-M model consistently produced reliable results, yielding higher KGE and NSE values for the Camastra basin, the Agri basin at Pertusillo and Ponte la Marmora, and the Basento basin at Campomaggiore. HYGRID-M provided the best performances in the Agri basin at Pertusillo and Ponte la Marmora. Overall, across the six pilot basins, HYGRID-M achieved acceptable and, in many cases, high NSE values, demonstrating the predictive strength of the proposed model. Optimal β values played a critical role in model calibration and overall performance. Across the Basilicata basins, β values were generally 0.7, demonstrating a degree of consistency. However, exceptions were observed for Agri at Pertusillo and Agri at Ponte la Marmora, where the optimal β was significantly lower, at 0.3, for both configurations. Moreover, the optimal β was obtained as 0.5 for Bradano at San Giuliano. These variations emphasized the localized nature of runoff generation processes and the importance

Table 2
Evaluation statistics for monthly average AET by HYGRID-M under heterogeneous and uniform soil conditions and BIGBANG against GLASS, ETMonitor and MOD16 datasets.

Data	R	KGE	RMSE (mm/month)
$AET_{HYGRID\text{-}M(heterogeneous)}$ - AET_{GLASS}	0.68	0.58	23.45
$AET_{HYGRID\text{-}M\ (uniform)}$- AET_{GLASS}	0.58	0.52	27.00
$AET_{BIGBANG\ (uniform)}$- AET_{GLASS}	0.73	0.44	26.86
$AET_{HYGRID\text{-}M(heterogeneous)}$ - $AET_{ETMonitor}$	0.75	0.72	19.19
$AET_{HYGRID\text{-}M\ (uniform)}$- $AET_{ETMonitor}$	0.66	0.65	22.37
$AET_{BIGBANG\ (uniform)}$- $AET_{ETMonitor}$	0.78	0.63	20.62
$AET_{HYGRID\text{-}M(heterogeneous)}$ - AET_{MOD16}	0.84	0.75	14.16
$AET_{HYGRID\text{-}M\ (uniform)}$- AET_{MOD16}	0.78	0.70	16.16
$AET_{BIGBANG\ (uniform)}$- AET_{MOD16}	0.78	0.69	16.33

Table 3
Kling–Gupta efficiency (KGE) and Nash-Sutcliffe efficiency (NSE) values associated with β for selected pilot basins.

#	Basins	A (km^2)	HYGRID-M (Heterogeneous)		
			KGE	NSE	β
1	Camastra (Basento)	341.90	0.46	0.67	0.7
2	Bradano at San Giuliano	1627.83	0.61	0.40	0.5
3	Bradano at Acerenza	143.00	0.52	0.66	0.7
4	Agri at Pertusillo	581.00	0.87	0.81	0.3
5	Agri at Ponte la Marmora	265.00	0.75	0.58	0.3
6	Basento at Campomaggiore	840.00	0.39	0.62	0.7
7	Arcidiaconata at Ponte Rapolla-Lavello (Ofanto)	125.68	0.47	0.41	0.7
8	Carapelle at Ponte Vecchio di Ordona	503.82	0.78	0.65	0.5
9	Volturno at Cancello Arnone	5558.00	0.79	0.75	0.3
10	Turbolo at Fitterizzi	7.01	0.70	0.76	0.5
11	Crati at Santa Sofia d'Epiro	1262.75	0.72	0.89	0.5

of parameter optimization.

In the Puglia region, analysis of two pilot basins revealed that the HYGRID-M model, provides good and consistent performance for the Carapelle basin at Ponte Vecchio di Ordona, demonstrating robustness despite variability in soil representation. Optimal β values further reflected these differences, with both soil conditions favoring 0.7 in Arcidaconata basin at Ponte Rapolla-Lavello and 0.5 in the Carapelle basin at Ponte Vecchio di Ordona.

The Campania region presented a different scenario. For the Volturno basin at Cancello Arnone, the HYGRID-M model delivered high KGE and NSE values. The optimal β value for this basin was 0.3, while performance metrics with $\beta = 0.5$ remain acceptable through lower than those achieved with $\beta = 0.3$.

Further assessments in the Calabria region, focusing on the Turbolo basin at Fitterizzi and the Crati basin at Santa Sofia, demonstrated consistent results. Both basins yielded high KGE and NSE values, confirming the adaptability of the model in varied environments. Optimal β values were 0.7 for both basins.

It should be noted that the HYGRID-M model generally provided reliable performance across the analyzed basins. Moreover, β remained a highly sensitive and region-specific parameter, requiring careful calibration to achieve optimal runoff estimation at the basin scale. Furthermore, the model robustness across diverse climatic and physiographic settings in Southern Apennines demonstrated the potential of the HYGRID-M model for broader application, provided parameterization strategies were adapted to the basin scale.

4. Discussion

The HYGRID-M model incorporated an updated evapotranspiration formulation based on the temperature-based Hargreaves equation with a regionalized coefficient, together with an explicit representation of soil heterogeneity and land use change across the simulation period, providing a more realistic description of land surface processes. Comparing to existing grid-based models, the structural refinements led to different partitioning in water balance calculations of the HYGRID-M model. This combined approach enhanced the model's responsiveness to climatic variability while maintaining low calibration dependence. This approach also enhanced the sensitivity to temperature variability, reduced the systematic underestimation of AET observed in BIGBANG, and improved the ability to capture the spatial and temporal variability in AET and Q estimates, particularly between mountainous and lowland areas. The significant agreement with multiple independent datasets indicated that incorporating spatial heterogeneity in soil properties within a monthly framework can substantially improve the model structure without intensive calibration approach.

The spatially heterogeneous Mediterranean basins dominated by AET and those generating substantial Q highlighted the role of soil storage heterogeneity in regulating water balance partitioning. Existing monthly grid-based water balance models typically assume uniform soil water storage, which limit the representation of climatic and geomorphological gradients. In the HYGRID-M model, the spatially heterogeneous storage capacity allowed precipitation inputs to be partitioned differently depending on local land surface characteristics, leading to a more differentiated hydrological response across the region. This confirmed that even within simplified monthly grid-based frameworks, introducing soil heterogeneity was essential to reproduce realistic Q generation patterns.

The comparatively limited interannual variability of AET relative to Q reflects the dominant control of evaporative demand in Mediterranean hydro-climates. Under these water-limited conditions, AET is largely constrained by atmospheric demand and soil moisture availability, whereas Q remained more sensitive to precipitation variability. The progressive increase in AET over the simulation period was therefore consistent with increasing temperature-driven atmospheric demand, which gradually reduced the fraction of water available for Q generation. This behavior is consistent with the conceptual understanding of water-limited regimes, where AET regulates long-term water availability while Q primarily reflects precipitation fluctuations.

The analysis indicated that the main improvement introduced by the HYGRID-M model did not arise from short-term variability in evapotranspiration formulations, but from the spatial representation of soil storage capacity, which governs how available water is redistributed over seasonal and interannual time scales. Differences between generalized and regionalized Hargreaves coefficients became less pronounced at monthly resolution due to temporal aggregation, suggesting that enhanced model structure in this framework was achieved primarily through structural representation of spatial controls rather than parameter tuning. This interpretation was supported by the comparison with global AET products, where the HYGRID-M model under heterogeneous soil conditions achieved R up to 0.84 and KGE up to 0.75, indicating that spatially variable soil storage improved AET estimates.

At the RBD scale, Q estimates remained physically consistent with precipitation forcing and showed comparable with BIGBANG estimates. At basin scale, the model successfully reproduced seasonal flow patterns and major flood events, with performance reaching KGE values up to 0.87 and NSE up to 0.89, based on observed discharge values from 11 pilot basins. These results confirmed the transferability of the model at the RBD scale to the basin scale. The sensitivity of Q to the coefficient β highlighted its role of a key parameter representing basin-scaled Q generation processes, such as impervious surfaces and soil saturation dynamics, rather than a purely empirical fitting coefficient. Basin-specific adjustment of β therefore reflected physical heterogeneity not resolved at RBD scale.

We have carried out the sensitivity analysis of the simulated components to key methodological assumptions. The analysis focused on the effects of: (i) soil water storage representation, comparing a uniform 1 m soil depth baseline with spatially heterogeneous soil depths; (ii) land use representation, considering both static and time-varying land use across the simulation period; and (iii) evapotranspiration parameterization, comparing the constant Hargreaves coefficient with a regionally calibrated coefficient. The analysis was conducted for the Southern Apennines District over the period 2000–2023. Compared to uniform soil depth assumptions, heterogeneous configurations improved agreement with reference AET datasets, reducing RMSE by ~3 mm month^{-1}, respectively, and yielding higher KGE values. Although district-scale runoff metrics exhibited limited sensitivity, Q varies by up to ~30% in response to soil depth, particularly in winter. Land use dynamics further affected both AET and Q, with monthly discharge variations reaching ~45%, whereas evapotranspiration parameterization had a comparatively minor impact, with differences of approximately 5%.

However, one of the limitations is that β in the HYGRID-M model was generally set to 0.5, even though it can vary depending on the extent of impervious surfaces and the characteristics of different climatic regions (Rautela et al., 2023). The simulations were performed using different β values ranging between 0.3 and 0.7. This variation indicated the necessity of calibrating β for each watershed individually to ensure an accurate runoff estimation. Additionally; c varies from 165 to 225 mm/^{0}C/ month (Rautela et al., 2023) and 50 to 180 mm/^{0}C/ month (USDA - United States Department of Agriculture, 2004). In this study; c was adopted based on the study of Braca and Ducci (2018); which may introduce uncertainty when applied to regions with differing climatic or snow conditions. Moreover; some empirical formulations were embedded in HYGRID-M; that might lead to potential uncertainty in the estimation of water balance components. Furthermore; since the model operated at the RBD scale; which encompassed diverse climatic regions; this broad spatial application can limit the accuracy of Q estimation due to regional variability in hydrological responses. In this study; the availability of direct observed Q at RBD scale is limited. Consequently; the evaluation of model performance relies exclusively on the BIGBANG model outputs which provide a spatially distributed monthly runoff dataset derived from a national-scale water balance framework.

Moreover; potential uncertainties may arise from the heterogeneous resolution of the input datasets. Climatic variables and other forcing data such as soil and land use were derived from sources with different native spatial resolutions and resampling procedures. These inconsistencies can reduce the internal coherence of the model forcing and potentially affect the simulation reliability. More uniform and harmonized datasets would improve the robustness of the model outputs. Furthermore; both soil characteristics and land-use conditions directly control water storage; evapotranspiration; and runoff generation processes; these uncertainties can propagate into the estimation of AET and Q; potentially influencing the spatial and temporal patterns reproduced by the model (Fox et al., 2012; Rautela et al., 2025a).

Future developments should include the automatic calibration of β and initial soil moisture conditions using machine learning or optimization algorithms to reduce parameter uncertainty and improve adaptability across watersheds. Extending HYGRID-M to different hydroclimatic contexts, comparing with other water balance models in those contexts and testing it under a range of climate scenarios will enable the assessment of future changes in AET and Q. Thus, HYGRID-M can evolve into a versatile platform for advancing sustainable water management and supporting policy decisions under changing climatic conditions.

5. Conclusions

This study presented HYGRID-M, a monthly grid-based hydrological model for estimating water-balance components at RBD scale while preserving structural simplicity and low calibration dependency. The main advantages of the model structure lie in: (i) explicit representation of soil heterogeneity derived from dynamic land use and (ii) a regionalized temperature-driven evapotranspiration formulation adapted to Mediterranean hydroclimatic conditions. The model was applied to the Southern Apennines District for the simulation period 2000–2023.

The representation of spatial heterogeneity in soil water storage substantially improved the model performance in estimating water balance components. AET estimates by the HYGRID-M under heterogeneous soil conditions exhibited better agreement with all independent global datasets with R up to 0.84 and KGE up to 0.75, outperforming both its uniform configuration and the BIGBANG model. Among all global datasets, MOD16 datasets were strongly consistent with annual average AET estimates by the model and monthly average percent differences yielding the narrowest variations varying from 0 to 30%. Meanwhile variations in β values (0.3, 0.5, and 0.7) or Hargreaves coefficients had minimal impact on modeled AET. This indicates that the main improvement arose from structural representation of spatial soil storage rather than from parameter tuning.

Q estimates at RBD scale were physically consistent with precipitation forcing and were comparable with those from the BIGBANG model. It is noted that estimation of Q at the RBD scale was sensitive to the spatial heterogeneity in soil properties, revealing more pronounced peaks under uniform soil conditions. Evaluating with the observed discharge from 11 pilot basins, the model outperformed eight out of eleven basins with KGE and NSE as high as 0.87 and 0.89. This indicates the transferability of the model to the basin scale with satisfactory performance. It is also noted that the β plays a key role in runoff generation at the basin scale.

Overall, the HYGRID-M model demonstrated that introducing spatial heterogeneity in soil properties in monthly grid-based framework enhanced the model performance without increasing the model complexity. This modeling strategy provides a practical bridge between simplified regional water balance models and more parameter-intensive distributed approaches, enabling large-scale hydrological assessment and supporting water resource management under changing climatic conditions.

CRediT authorship contribution statement

Htay Htay Aung: Writing – original draft, Visualization, Validation, Software, Methodology, Investigation, Formal analysis, Data curation, Conceptualization. **Biagio Sileo:** Visualization, Validation, Data curation, Conceptualization. **Mauro Fiorentino:** Supervision, Resources, Conceptualization. **Silvano Fortunato Dal Sasso:** Writing – review & editing, Validation, Supervision, Resources, Project administration, Methodology, Investigation, Funding acquisition, Formal analysis, Data curation.

Funding

The present research has been carried out within the RETURN Extended Partnership and received funding from the European Union Next-GenerationEU (National Recovery and Resilience Plan—NRRP, Mission 4, Component 2, Investment 1.3, SPOKE VS1-Acqua, PE0000005) under the cascading funding scheme WaterWISE-Water Management Strategies and Climate Change Adaptation in Southern Italy.

Declaration of competing interest

The authors declare the following financial interests/personal relationships which may be considered as potential competing interests: Silvano F. Dal Sasso reports financial support was provided by European Union Next-GenerationEU. If there are other authors, they declare that they have no known competing financial interests or personal relationships that could have appeared to influence the work reported in this paper.

Acknowledgements

The authors wish to sincerely thank the project members for their valuable support in providing the runoff data from the pilot basins.

Appendix A. Supplementary data

Supplementary data to this article can be found online at https://doi.org/10.1016/j.catena.2026.110175.

Data availability

The authors do not have permission to share part of the data.

References

Abdollahi, K., Bashir, I., Verbeiren, B., Haroun, M.R., Griensven, A.V., Huysmans, M., Batelaa, O., 2017. A distributed monthly water balance model: formulation and application on black Volta basin. Environ. Earth Sci. 76 (198), 1–18. https://doi.org/10.1007/s12665-017-6512-1.

Amiri, M., Salem, A., Ghzal, M., 2022. Spatial-temporal water balance components estimation using integrated GIS-based Wetspass-M model in Moulouya basin, Morocco. ISPRS Int. J. Geo Inf. 11 (2), 139. https://doi.org/10.3390/ijgi11020139.

Arnold, J.G., Muttiah, R.S., Srinivasan, R., Allen, P.M., 2000. Regional estimation of base-flow and groundwater recharge in the upper Mississippi river basin. J. Hydrol. 227 (1–4), 21–40. https://doi.org/10.1016/S0022-1694(99)00139-0.

Ballabio, C., Panagos, P., Monatanarella, L., 2016. Mapping topsoil physical properties at European scale using the LUCAS database. Geoderma 261, 110–123. https://doi.org/10.1016/j.geoderma.2015.07.006.

Batelaan, O., De Smedt, F., 2001. Wetspass: a flexible, GIS based, distributed recharge methodology for regional groundwater. In: Impact of Human Activity on Groundwater Dynamics: Proceedings of an International Symposium (Symposium S3) Held During the Sixth Scientific Assembly of the International Association of Hydrological Sciences (IAHS) at Maastricht, The Netherlands, from 18 to 27 July 2001, Number 269, p. 11.

Bergström, S., 1975. The development of a snow routine for the HBV-2 model. Hydrol. Res. 6 (2), 73. https://doi.org/10.2166/nh.1975.0006.

Boughton, W.C., 1987. Evaluating partial areas of watershed runoff. J. Irrig. Drain. Eng. 113 (3), 356–366. https://doi.org/10.1061/(ASCE)0733-9437(1987)113:3(356).

Braca, G., Ducci, D., 2018. Development of a GIS based procedure (BIGBANG 1.0) for evaluating groundwater balances at national scale and comparison with

groundwater resources evaluation at local scale. In: Groundwater and Global Change in the Western Mediterranean Area. springer international publishing, Cham, pp. 53–61.
Braca, G., Bussettini, M., Ducci, D., Lastoria, B., Mariani, S., 2019. Evaluation of national and regional groundwater resources under climate change scenarios using a GIS-based water budget procedure. Rend. Lincei-Sci. Fis. 30 (1), 109–123. https://doi.org/10.1007/s12210-018-00757-6.
Braca, G., Bussettini, M., Gafà, R.M., Monti, G.M., Martarelli, L., Silvi, A., La Vigna, F., 2022. The nationwide water budget estimation in the light of the new permeability map of Italy. Acque Sotter. Ital. J. Groundw. 3, 31–39. https://doi.org/10.7343/as-2022-575.
Cleugh, H.A., Leuning, R., Mu, Q., Running, S.W., 2007. Regional evaporation estimates from flux tower and MODIS satellite data. Remote Sens. Environ. 106 (3), 285–304. https://doi.org/10.1016/j.rse.2006.07.007.
Dal Sasso, S.F., Pizarro, A., Onorati, B., Margiotta, M.R., Zeng, Y., Su, Z., Manfreda, S., Fiorentino, M., 2025. Assessing the performance of single and multi-criteria calibration approaches for hydrological modelling: a comparative analysis. Hydrol. Sci. J. 70 (16), 3115–3130.
Fox, D.M., Witz, E., Blanc, V., Soulié, C., Penalver-Navarro, M., Dervieux, A., 2012. A case study of land cover change (1950–2003) and runoff in a Mediterranean catchment. Appl. Geogr. 32 (2), 810–821. https://doi.org/10.1016/j.apgeog.2011.07.007.
Grogan, D.S., Zuidema, S., Prusevich, A., Wollheim, W.M., Glidden, S., Lammers, R.B., 2022. Water balance model (WBM) v. 1.0. 0: a scalable gridded global hydrologic model with water-tracking functionality. Geosci. Model Dev. 15 (19), 7287–7323. https://doi.org/10.5194/gmd-15-7287-2022.
Gupta, H.V., Kling, H., Yilmaz, K.K., Martinez, G.F., 2009. Decomposition of the mean squared error and NSE performance criteria: implications for improving hydrological modelling. J. Hydrol. 377 (1–2), 80–91. https://doi.org/10.1016/j.jhydrol.2009.08.003.
Hargreaves, G.H., Samani, Z.A., 1985. Reference crop evapotranspiration from temperature. Appl. Eng. Agric. 1 (2), 96–99. https://doi.org/10.13031/2013.26773.
Hlavčová, K., Szolgay, J., Kohnova, S., Hlásny, T., 2008. Simulation of hydrological response to the future climate in the Hron river basin. J. Hydrol. Hydromech. 56 (3), 163–175.
Hock, R., 1999. A distributed temperature-index ice-and snowmelt model including potential direct solar radiation. J. Glaciol. 45 (149), 101–111. https://land.copernicus.eu/en/products/corine-land-cover/clc2018 (accessed on 28 September 2025).
Kumar, M., Tiwari, R.K., Kumar, K., Rautela, K.S., Safi, S., 2024. Quantitative analysis of hydropower potential in the upper Beas basin using geographical information system and MIKE 11 nedbor afrstromnings model (NAM). Ecohydrol 17 (4), e2618. https://doi.org/10.1002/eco.2618.
Liang, X., Lettenmaier, D.P., 1994. A simple hydrologically based model of land surface water and energy fluxes forgeneral circulation models. J. Geophys. Res. 99 (D7), 14415–14428. https://doi.org/10.1029/94JD00483.
Liu, Y.B., De Smedt, F., 2004. WetSpa Extension: Documentation and User Manual. Department of Hydrology and Hydraulic Engineering, Vrije Universiteit Brussel, Belgium.
Longobardi, A., Villani, P., Grayson, R., Western, A., 2003. On the relationship between runoff coefficient and catchment initial conditions. In: Proceedings of MODSIM, pp. 867–872.
Mammoliti, E., Fronzi, D., Mancini, A., Valigi, D., Tazioli, A., 2021. WaterbalANce, a webapp for Thornthwaite–Mather water balance computation: comparison of applications in two European watersheds. Hydrology 8 (1), 34. https://doi.org/10.3390/hydrology8010034.
Mariotti, A., Zeng, N., Yoon, J.H., Artale, V., Navarra, A., Alpert, P., Li, L.Z., 2008. Mediterranean water cycle changes: transition to drier 21st century conditions in observations and CMIP3 simulations. Environ. Res. Lett. 3 (4), 044001. https://doi.org/10.1088/1748-9326/3/4/044001.
McCabe, G.J., Markstrom, S.L., 2007. A monthly water-balance model driven by a graphical user interface (No. 2007-1088). US Geological Survey.
McCabe, G.J., Wolock, D.M., 2011. Independent effects of temperature and precipitation on modeled runoff in the conterminous United States. Water Resour. Res. 47 (11). https://doi.org/10.1029/2011WR010630.
Mendicino, G., Senatore, A., 2013. Regionalization of the hargreaves coefficient for the assessment of distributed reference evapotranspiration in southern Italy. J. Irrig. Drain. Eng. 139 (5), 349–362. https://doi.org/10.1061/(ASCE)IR.1943-4774.0000547.
Mizukami, N., Rakovec, O., Newman, A.J., Clark, M.P., Wood, A.W., Gupta, H.V., Kumar, R., 2019. On the choice of calibration metrics for “high-flow” estimation using hydrologic models. Hydrol. Earth Syst. Sci. 23, 2601–2614. https://doi.org/10.5194/hess-23-2601-2019.
Mu, Q., Heinsch, F.A., Zhao, M., Running, S.W., 2007. Development of a global evapotranspiration algorithm based on MODIS and global meteorology data. Remote Sens. Environ. 111 (4), 519–536. https://doi.org/10.1016/j.rse.2007.04.015.
Mu, Q., Zhao, M., Running, S.W., 2011. Improvements to a MODIS global terrestrial evapotranspiration algorithm. Remote Sens. Environ. 115 (8), 1781–1800. https://doi.org/10.1016/j.rse.2011.02.019.
Nash, J.E., Sutcliffe, J.V., 1970. River flow forecasting through. Part I. A conceptual models discussion of principles. J. Hydrol. 10 (3), 282–290. https://doi.org/10.1016/0022-1694(70)90255-6.
Pechlivanidis, I.G., Jackson, B.M., Mcintyre, N.R., Wheater, H.S., 2011. Catchment scale hydrological modelling: A review of model types, calibration approaches and uncertainty analysis methods in the context of recent developments in technology and applications. Global NEST journal 13 (3), 193–214.
Peres, D.J., Bonaccorso, B., Palazzolo, N., Cancelliere, A., Mendicino, G., Senatore, A., 2023. A dynamic approach for assessing climate change impacts on drought: an analysis in southern Italy. Hydrol. Sci. J. 68 (9), 1213–1228. https://doi.org/10.1080/02626667.2023.2217332.
Rautela, K.S., Kumar, D., Gandhi, B.G.R., Kumar, A., Dubey, A.K., Khati, B.S., 2023. Evaluating hydroelectric potential in alaknanda basin, Uttarakhand using the snowmelt runoff model (SRM). J. Water Clim. Chang. 14 (11), 4146–4161. https://doi.org/10.2166/wcc.2023.341.
Rautela, K.S., Kuniyal, J.C., Goyal, M.K., Kanwar, N., Bhoj, A.S., 2024. Assessment and modelling of hydro-sedimentological flows of the eastern river Dhauliganga, north-western Himalaya, India. Nat. Hazards 120, 5385–5409. https://doi.org/10.1007/s11069-024-06413-7.
Rautela, K.S., Kanwar, N., Kuniyal, J.C., Sofi, M.S., Goyal, M.K., Bhoj, A.S., Singh, H.B., 2025a. Assessing hydro-climatological variability and land use characteristics of the headwater basins of the indian Himalayan region. Earth Syst. Environ. 9, 2211–2233. https://doi.org/10.1007/s41748-025-00662-7.
Rautela, K.S., Gupta, V., Devi, J.P., Majeed, L.R., Kuniyal, J.C., 2025b. Modeling stage-discharge and sediment-discharge relationships in data-scarce Himalayan river basin Dhauliganga, Central Himalaya, using neural networks. CLEAN–Soil Air Water 53 (1), 2300388. https://doi.org/10.1002/clen.202300388.
Running, S., Mu, Q., Zhao, M., Moreno, A., 2021. MODIS/Terra Net Evapotranspiration Gap-Filled 8-day L4 Global 500m SIN Grid V061. NASA EOSDIS Land Processes Distributed Active Archive Center (DAAC) Data Set, MOD16A2GF-061 [dataset]. https://doi.org/10.5067/MODIS/MOD16A2GF.061.
Saxton, K.E., Rawls, W.J., 2006. Soil water characteristic estimates by texture and organic matter for hydrologic solutions. Soil Sci. Soc. Am. J. 70 (5), 1569–1578. https://doi.org/10.2136/sssaj2005.0117.
Senatore, A., Mendicino, G., Smiatek, G., Kunstmann, H., 2011. Regional climate change projections and hydrological impact analysis for a mediterranean basin in southern Italy. J. Hydrol. 399 (1–2), 70–92. https://doi.org/10.1016/j.jhydrol.2010.12.035.
Senatore, A., Mendicino, G., Cammalleri, C., Ciraolo, G., 2015. Regional-scale modeling of reference evapotranspiration: Intercomparison of two simplified temperature-and radiation-based approaches. J. Irrig. Drain. Eng. 141 (12), 04015022. https://doi.org/10.1061/(ASCE)IR.1943-4774.0000917.
Senatore, A., Parrello, C., Almorox, J., Mendicino, G., 2020. Exploring the potential of temperature-based methods for regionalization of daily reference evapotranspiration in two Spanish regions. J. Irrig. Drain. Eng. 146 (3), 05020001. https://doi.org/10.1061/(ASCE)IR.1943-4774.000144.
Thomas Jr., H.A., 1981. Improved methods for national water assessment, water resources contract: WR15249270. Harvard Water Resources Group.
Thornthwaite, C.W., 1948. An approach toward a rational classification of climate. Geogr. Rev. 38 (1), 55–94. https://doi.org/10.2307/210739.
Tóth, G., Jones, A., Montanarella, L., Alewell, C., Ballabio, C., Carre, F., De, B.D., Guicharnaud, R.A., Gardi, C., Hermann, T., Meusburger, K., et al., 2013. LUCAS Topoil Survey-Methodology, Data and Results. Publications Office of the European Union, Luxembourg. https://doi.org/10.2788/97922.
USDA - United States Department of Agriculture, 2004. Chapter 11 Snowmelt. In: Part 630 Hydrology National Engineering Handbook.
Wang, Q., Pagano, T., Zhou, S., Hapuarachchi, H., Zhang, L., Robertson, D., 2011. Monthly versus daily water balance models in simulating monthly runoff. J. Hydrol. 404 (3–4), 166–175. https://doi.org/10.1016/j.jhydrol.2011.04.027.
Wieczorek, M.E., Signell, R.P., McCabe, G.J., Wolock, D.M., 2022. USGS Monthly Water Balance Model Inputs and Outputs for the Conterminous United States, 1895-2020, Based on ClimGrid Data: U.S. Geological Survey Data Release. https://doi.org/10.5066/P9JTV1T6.
Wolock, D.M., McCabe, G.J., 1999. Explaining spatial variability in mean annual runoff in the conterminous United States. Clim. Res. 11 (2), 149–159. https://doi.org/10.3354/cr011149.
Xiao, M., Gao, M., Vogel, R.M., Lettenmaier, D.P., 2020. Runoff and evapotranspiration elasticities in the western United States: are they consistent with dooge’s complementary relationship? Water Resour. Res. 56 (8). https://doi.org/10.1029/2019WR026719 e2019WR026719.
Xie, Z., Yao, Y., Zhang, X., Liang, S., Fisher, J.B., Chen, J., Jia, K., Shang, K., Yang, J., Yu, R., Guo, X., 2022. The global land surface satellite (GLASS) evapotranspiration product version 5.0: algorithm development and preliminary validation. J. Hydrol. 610, 127990. https://doi.org/10.1016/j.jhydrol.2022.127990.
Xu, C.Y., Singh, V.P., 1998. A review on monthly water balance models for water resources investigations. Water Resour. Manag. 12 (1), 20–50. https://doi.org/10.1023/a:1007916816469.
Zhang, L., Potter, N., Hickel, K., Zhang, Y., Shao, Q., 2008. Water balance modeling over variable time scales based on the budyko framework–model development and testing. J. Hydrol. 360 (1–4), 117–131. https://doi.org/10.1016/j.jhydrol.2008.07.021.
Zheng, C., Jia, L., Hu, G., 2022a. Global land surface evapotranspiration monitoring by ETMonitor model driven by multi-source satellite earth observations. J. Hydrol. 613, 128444. https://doi.org/10.1016/j.jhydrol.2022.128444.
Zheng, C., Jia, L., Hu, G., 2022b. ETMonitor Global Actual Evapotranspiration Dataset with 1-km Resolution. National Tibetan Plateau / Third Pole Environment Data Center [dataset]. https://doi.org/10.11888/RemoteSen.tpdc.272831.